

# GEMeX: A Large-Scale, Groundable, and Explainable Medical VQA Benchmark for Chest X-ray Diagnosis

Bo Liu<sup>1</sup>, Ke Zou<sup>2,3</sup>, Liming Zhan<sup>1</sup>, Zexin Lu<sup>1</sup>, Xiaoyu Dong<sup>1</sup>, Yidi Chen<sup>4</sup>, Chengqiang Xie<sup>1</sup>, Jiannong Cao<sup>1</sup>, Xiao-Ming Wu<sup>1\*</sup>, Huazhu Fu<sup>5\*</sup>

<sup>1</sup>The Hong Kong Polytechnic University, Hong Kong, <sup>2</sup>National University of Singapore, Singapore,

<sup>3</sup>Sichuan University, China, <sup>4</sup>West China Hospital of Sichuan University, China

<sup>5</sup>Institute of High Performance Computing, Agency for Science, Technology and Research, Singapore

## Abstract

Medical Visual Question Answering (VQA) is an essential technology that integrates computer vision and natural language processing to automatically respond to clinical inquiries about medical images. However, current medical VQA datasets exhibit two significant limitations: (1) they often lack visual and textual explanations for answers, which impedes their ability to satisfy the comprehension needs of patients and junior doctors; (2) they typically offer a narrow range of question formats, inadequately reflecting the diverse requirements encountered in clinical scenarios. These limitations pose significant challenges to the development of a reliable and user-friendly Med-VQA system. To address these challenges, we introduce a large-scale, **Groundable**, and **Explainable Medical VQA** benchmark for chest X-ray diagnosis (GEMeX), featuring several innovative components: (1) A multi-modal explainability mechanism that offers detailed visual and textual explanations for each question-answer pair, thereby enhancing answer comprehensibility; (2) Four distinct question types—open-ended, closed-ended, single-choice, and multiple-choice—that better reflect diverse clinical needs. We evaluated 10 representative large vision language models on GEMeX and found that they underperformed, highlighting the dataset’s complexity. However, after fine-tuning a baseline model using the training set, we observed a significant performance improvement, demonstrating the dataset’s effectiveness. The project is available at [www.med-vqa.com/GEMeX](http://www.med-vqa.com/GEMeX).

## 1. Introduction

Large vision language models (LVLMs) have recently achieved huge breakthroughs in artificial intelligence [1, 2, 5, 11, 35, 38, 55, 57], demonstrating remarkable capabilities in understanding visual content while generating coherent

\* Corresponding author.

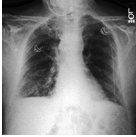
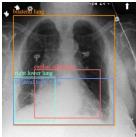
Dataset	VQA Type	Example
 MIMIC-CXR-VQA	Closed-ended	<b>Closed-ended VQA:</b> Q: Is any devices present within the right atrium? A: No.
	Open-ended	<b>Open-ended VQA:</b> Q: What are all the diseases identifiable within the right hilar structures? A: A small right pleural effusion.
 Ours	Closed-ended	<b>Multi-choice VQA:</b> Q: Which regions on the X-ray show signs of abnormalities? C: ["A: Bilateral lungs", "B: Right costophrenic angle", "C: Bilateral lower lung", "D: Cardiac region"] A: ["A", "B", "C", "D"] Reason: Abnormalities are seen in the bilateral lungs (hyperinflation), right costophrenic angle (blunting), bilateral lower lung (atelectasis), and cardiac silhouette (enlargement). Bounding box: [[28, 40, 167, 190], [28, 124, 85, 184], [28, 126, 165, 189], [57, 114, 147, 180]]
	Open-ended	
	Single-choice	
	Multi-choice	

Figure 1. Our GEMeX stands out from existing medical VQA datasets by providing diverse question types, detailed textual explanations, and visual groundings.

ent natural language responses. These advancements have driven innovations across various domains [13, 15, 47], with healthcare emerging as a key application. Within this domain, medical visual question answering (Med-VQA) stands out as a crucial task which automatically provides reliable and user-friendly answers [29] to questions about medical images [24], facilitating healthcare professionals in diagnosis, medical education, and clinical decision-making.

To ensure the reliability and user-friendliness of Med-VQA systems, it is crucial to incorporate answer explanations along with a diverse set of question formats. Although significant progress has been made by existing Med-VQA systems [16, 18, 24, 31, 53], none have yet integrated answer explanations. As emphasized by Li et al. (2018), explanations are as essential as the answers themselves in general VQA systems. This holds even stronger in the context of medical VQA, where the domain-specific nature of the task amplifies the need for clarity [24]. If Med-VQA tools are to assist in clinical processes, the datasets must be

Dataset	# Images	# QA Pairs	# Modalities	# Question Types‡	# Groundable	# Explainable
VQA-RAD [24]	0.315K	3.5K	Diverse†	O. & C.	✗	✗
SLAKE [31]	0.642K	14K	Diverse†	O. & C.	✗	✗
OmniMedVQA [18]	118.010K	128K	Diverse†	O. & C. & S.	✗	✗
PMC-VQA [53]	149.075K	227K	Diverse†	O. & C. & S.	✗	✗
VQA-Med [6]	4.5K	4.5K	Diverse†	O. & C.	✗	✗
PathVQA [16]	149K	33K	Pathology	O. & C.	✗	✗
RadGenome-Chest CT [54]	50.188K	1.3M	Chest CT	O. & C.	✓	✗
MIMIC-Diff-VQA [17]	164.324K	700K	Chest X-ray	O. & C.	✗	✗
MIMIC-CXR-VQA [4]	142.797K	377K	Chest X-ray	O. & C.	✗	✗
<b>GEMeX (Ours)</b>	151.025K	1.6M	Chest X-ray	O. & C. & S. & M.	✓	✓ (Vision & Language)

Table 1. Comparison of medical VQA Datasets. † indicates a composition of multiple body parts (e.g., head, chest, abdomen) and various image modalities (e.g., CT, MRI, X-ray, pathology). In the # Question Types‡ column, O., C., S., and M. represent “Open-ended”, “Closed-ended”, “Single-choice”, and “Multi-choice”, respectively.

designed to include explanations, so as to enhance patient comprehension and support the learning of junior medical practitioners. Additionally, the limited range of question formats, such as the absence of multiple-choice questions, restricts the real-world applicability and impairs the overall user-friendliness of medical AI systems.

To tackle the aforementioned challenges, we develop a large-scale, **Groundable**, and **Explainable Medical VQA** benchmark for chest X-ray diagnosis (GEMeX). We first undertake a comprehensive data refinement process upon the Chest ImaGenome dataset [45]. By collaborating with radiologists, we systematically redefine anatomical regions and establish more precise visual-text correspondence mappings, resulting in accurate region-grounded reports for each X-ray image. Subsequently, we leverage GPT-4o [1] to generate a diverse set of questions based on these grounded reports, covering four categories: open-ended, closed-ended, single-choice, and multiple-choice questions. Each question-answer pair is enriched with explicit reasoning and corresponding visual region annotations, as illustrated in Figure 1. The resulting dataset comprises 151,025 radiographic images and 1,605,575 questions. To our knowledge, this is currently the largest chest X-ray VQA dataset and the first Med-VQA dataset that simultaneously includes both textual and visual explanations.

We evaluate 10 representative LVLMs, including 5 from the general domain (e.g., LLaVA-v1 [35], Mini-GPT4-v1 [57], GPT-4o-mini [1]), and 5 from the medical domain (e.g., LLaVA-Med [26], XrayGPT [40], RadFM [43]). The experimental findings underscore the challenging characteristics of our dataset. Additionally, we propose a simple instruction-tuning strategy that derives a task-specific LLM. The impressive performance improvement highlights the effectiveness of our dataset. For evaluation, we develop three metrics to assess the accuracy of model outputs in terms of answers, reasoning, and visual grounding (localization generation). Notably, we apply both semantics-level score and gram-based metrics for natural language generation (e.g., BLEU and ROUGE). Re-

sults indicate that for models without GEMeX fine-tuning, semantics-level scoring is more reliable. After fine-tuning, however, the natural language generation metrics can better reflect the model’s understanding of the dataset.

The contributions of this paper can be summarized as follows:

- We introduce GEMeX, a large-scale Med-VQA dataset for chest X-rays, designed to support diverse question types and provide enhanced explainability for medical VQA systems. To our knowledge, it is the largest chest X-ray VQA dataset and the first Med-VQA dataset to embody the concept of multimodal explainability.
- We systematically benchmark 10 representative LVLMs using GEMeX, introducing multiple evaluation metrics to comprehensively demonstrate the performance of current popular LVLMs on the Med-VQA task.
- We show that our proposed precise vision-text explainability notably enhances the visual reasoning ability of LVLMs through fine-tuning, addressing a key deficiency observed in various models. We highlight the importance of a large-scale, groundable, and explainable VQA benchmark for advancing the development and deployment of LVLMs in healthcare.

## 2. Related Work

In this section, we review prior work relevant to our study, focusing on two main areas: existing datasets for Med-VQA and current methodologies developed for Med-VQA task.

### 2.1. Medical VQA Datasets

In recent years, various datasets have been created to advance medical VQA research, each tackling specific challenges across clinical domains. A detailed comparison to other VQA datasets can be seen in Table 1. Specifically, VQA-RAD [24] is a pioneer dataset that offers over 3,000 question-answer pairs focused on radiology images. SLAKE [31] is the first manually created dataset with over 14,000 QA pairs across CT, MRI, and X-ray images, enabling models to handle complex scenarios by combining

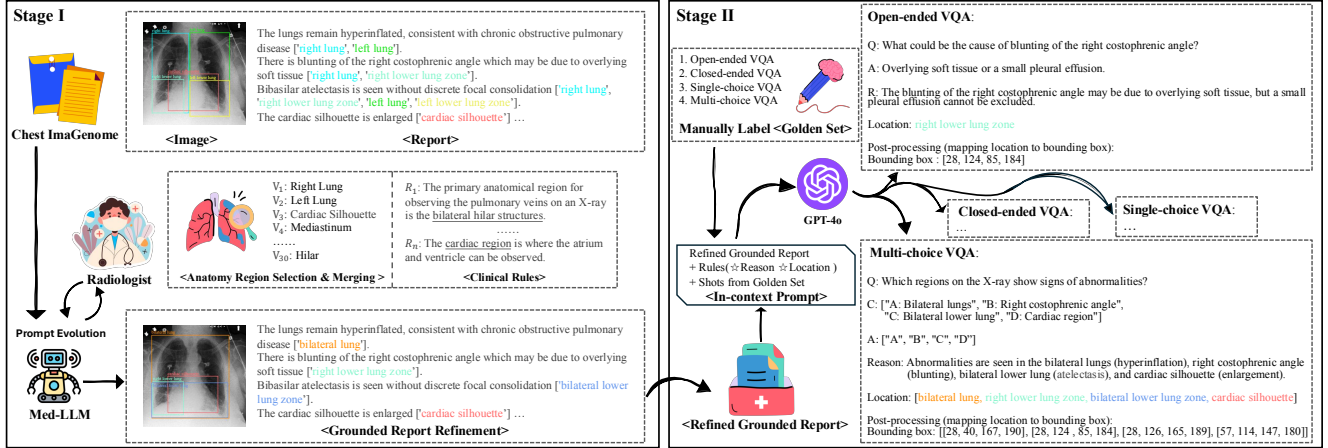


Figure 2. Illustration of the proposed pipeline for constructing GEMeX, with two main stages. Stage I involves cleaning data from Chest ImaGenome, while Stage II designs prompts to enable GPT-4o to generate a large-scale, groundable, and explainable VQA dataset.

visual and textual information. VQA-Med [6] is a key dataset for Med-VQA competitions, with 4,500 radiology images and paired QA sets for training, validation, and testing. OmniMedVQA [18] provides more data and more imaging modalities, which cover the entire body, to encourage model generalization. PMC-VQA [53] generates VQA data by prompting a large language model to decompose captions of biomedical figures, enabling academic knowledge extraction. PathVQA [16] supplies over 32,000 QA pairs on histopathological images for fine-grained pathology analysis. Despite this diversity, these datasets collectively have fewer than 40K X-ray-related QA pairs, which may limit their utility for LVLm training.

For specialized tasks, RadGenome-Chest CT [54] supports chest CT diagnostics, while MIMIC-Diff-VQA [17] emphasizes differential diagnosis reasoning between two X-rays. MIMIC-CXR-VQA [4] expands MIMIC-CXR [21] with diverse question templates to generate thoracic radiology QA pairs, aiding in chest abnormality detection. However, all current datasets lack explainability and diverse question formats. They do not provide detailed visual and textual explanations for answers, which limits their usability for patient and junior doctor comprehension. Additionally, limited question types restrict their ability to simulate the variety of inquiries encountered in practice.

## 2.2. Medical VQA Methods

Inspired by the advancements in general VQA, medical VQA has gained significant traction as a specialized domain. Due to data limitations, however, most approaches [14, 22, 24, 30, 32, 36, 46, 50] have focused on directly embedding visual and textual information jointly to capture their relationships. With the rise of contrastive language-image pertaining (CLIP) [37], methods [8, 9, 12, 49, 51] start to focus on applying CLIP to Med-VQA.

A promising way is to fine-tune CLIP’s joint embeddings to better handle specific medical domains, enhancing the model’s understanding of clinical questions and visual features [28]. Recently, the explosion of large vision language models (LVLms) has further pushed the boundaries of medical domain [3, 25, 26, 40, 43, 58]. Generally, they first pre-train models on a large-scale image-text dataset (like PMC-OA [28], PMC-15M [51]) to map visual features into language model’s embedding space and then further tune with instruction data for medical consultation [3, 35] or disease diagnosis [7, 40, 42, 56]. These models are now leveraged for Med-VQA tasks to provide richer, more context-aware answers, extending beyond simple text-image alignment to incorporate broader knowledge-based reasoning.

Despite these advances, current methods are limited by the size and diversity of available datasets. Furthermore, the absence of detailed explanations in these datasets also hinders progress in building explainable VQA models, highlighting the need for methods and datasets that focus on explainability and clinical relevance.

## 3. Construction of GEMeX

We will elaborate on the construction of the proposed GEMeX dataset, accompanied by a schematic overview in Figure 2. The structure of this section is organized as follows: In Section 3.1, we introduce the initial step of dataset construction, focusing on refining anatomical regions and grounding reports; Section 3.2 covers the generation process for four distinct types of Med-VQA, incorporating multimodal explainability across both visual and textual dimensions. More details can be found in the Appendix.

### 3.1. Grounded Report Refinement

As shown in stage I of Figure 2, we build upon Chest ImaGenome [45] to construct our dataset, but with an emphasis on the mapping precision between visual regions and textually described entities. The emergence of Chest ImaGenome has led to significant advances in various multi-modal tasks, including Med-VQA [17] and grounded report generation [39]. However, after consulting radiologists, we find that the anatomical descriptions of regions of interest in ImaGenome are imprecise and lack simplicity, and they even introduce ambiguity into clinical diagnoses. Specifically, in ImaGenome, one sentence may be filled with multiple anatomical regions, *e.g.*, sentence “There is blunting of the right costophrenic angle which may be due to overlying soft tissue” corresponds to [“right lung”, “right lower lung zone”]. This drawback poses challenges in training models to precisely visual grounding. Therefore, in the first stage of construction, we perform sentence-region refinement, generating pairs where each sentence is associated with only one clinically precise textual region entity.

#### 3.1.1. Anatomical Region Selection and Merging

In the original Chest ImaGenome, there are 29 significant pathological regions. However, in alignment with radiologists’ practices, our dataset focuses on retaining core clinical regions that are crucial for diagnosing diseases through X-rays, such as the “left lower lung” and “mediastinum”. Less significant or marginal areas are excluded to streamline the diagnostic training process and enhance clinical relevance. For example, we exclude terms like “carina” which is not considered a core region, and “clavicle” which accounts for only about 2% of the total regional frequency. Furthermore, to enhance clarity and ensure that each sentence corresponds to a single pathological region with finer granularity, semantically similar regions are merged. For example, the “left lower lung zone” and “right lower lung zone” are combined into a “bilateral lower lung zone”. This consolidation aligns with conditions like “bibasilar atelectasis”, as illustrated in Stage I of Figure 2, where the condition is described as “Bibasilar atelectasis is seen without discrete focal consolidation”. In total, we define 30 anatomical regions eventually. Detailed transformation from Chest ImaGenome to ours can be found in the Appendix.

#### 3.1.2. Refinement with Medical LLM

After defining anatomical regions, we utilize OpenBioLLM-70B<sup>1</sup>, known for its outstanding performance across various medical NLP tasks, to refine original sentence-region pairs. To test the effectiveness of the prompt, we begin by randomly selecting 100 pairs from the Chest ImaGenome test set, which includes approximately 367 sentences. Initially, the performance

of the OpenBioLLM-70B model is suboptimal due to two main reasons: (1) some disease observation areas are not sufficiently detailed, as OpenBioLLM is an NLP model that lacks clinical expertise, and (2) when a sentence involves multiple regions that cannot be merged, the model may either output multiple regions or arbitrarily select one.

To address these limitations, we employ an iterative approach, gradually incorporating guidance (clinical rules) from radiologists and manually-labeled such cases, to effectively split and rewrite sentences. For example, “The cardiomeastinal silhouette is normal.” can be segmented into {“The cardiac silhouette is normal.”:“cardiac silhouette”, “The mediastinal silhouette is normal.”:“mediastinum”}, where “cardiomeastinal” corresponds to the “cardiac silhouette” and “mediastinum”. This approach ensures that the output clauses align one-to-one with the respective regions. Ultimately, the final prompt is determined with an accuracy of approximately 98.4% on the aforementioned test set. Part of the clinical rules can be seen in Stage I of Figure 2, and the complete prompt is outlined in the Appendix.

### 3.2. Groundable and Explainable VQA Generation

Although there are many Med-VQA datasets [4, 17] available, some even generated using MIMIC-CXR or Chest ImaGenome, they all have two weaknesses that diminish their practicality: (1) these datasets often lack strong explainability. When patients ask medical questions, the system may provide only simple textual explanations but without offering visually relevant guidance. This limitation can hinder the user’s understanding of the medical information presented; (2) the types of questions included in these datasets are limited, typically restricted to open-ended or closed-ended formats, with no inclusion of choice-based questions. This significantly restricts the flexibility and comprehensiveness of the datasets in addressing a broader spectrum of user inquiries. In general, these issues highlight the necessity for more versatile and explainable Med-VQA datasets to enhance their utility in clinical settings.

As shown in Stage II of Figure 2, we prepare to generate our VQA dataset after refining the grounded reports. Here, we employ GPT-4o [1] as a generator due to its remarkable capabilities in understanding and generating long texts. To enhance the quality of the generated questions and better align them with our objectives, we manually craft questions for 30 images according to their paired grounded report (as a golden set) to serve as demonstrations in the prompt for in-context learning. Moreover, we also design specific rules (like not generating questions that need to be answered by comparing two images) to ensure the quality of generated VQAs. For each image-report sample, we instruct the GPT-4o to generate a total of 11 questions: 3 open-ended VQAs, 2 closed-ended VQAs, 3 single-choice questions, and 3 multi-choice questions, culminating in ap-

<sup>1</sup><https://huggingface.co/aaditya/Llama3-OpenBioLLM-70B>

`messages = [{"role": "system", "content":`

`f" You are a chest X-ray AI assistant, and you are seeing a frontal view chest X-ray image, described by several phrases with visual regions. Generate 3 open-ended questions, 2 closed-ended questions, 3 single-choice questions, and 3 multi-choice questions about this chest X-ray. Format your output in JSON format.`

`Here are some rules:`

`(1) Include questions asking about the visual content of the image, containing abnormality, disease, location, severity, cause of disease, etc. For a CXR, the types of questions generated need to be diverse. Do not ask any questions that cannot be answered confidently.`

`(2) For each question, provide the answer, explain the reason for obtaining such answer, and output the corresponding visual regions as a visual clue.`

`(3) For open-ended questions, the answers must be concise. You should generate detailed reasons based on the provided CXR phrases and your medical knowledge. Do not refer to the text description in your questions or answers.`

`(4) Avoid questions that cannot be answered by looking at the given CXR image itself, such as asking about changes/comparisons from previous scans, asking about staff notifications, or asking about view types or other scans.`

`Here is one example:`

`Chest X-ray: {...}, One open-ended question can be: {...}, One closed-ended question can be: {...}, One single-choice question can be: {...}, One multi-choice question can be: {...}`

`messages += [{"role": "user", "content": "Chest X-ray: There is also fullness of the right hilum which is new. [visual location: right hilar structures] ..."}]`

Table 2. Our designed prompt for generating groundable and explainable medical VQA, using a grounded report as input.

	Open. (T/B)	Closed. (T/B)	Single. (T/B)	Multi. (T/B)
Train	441,471/466,725	272,323/277,249	441,114/448,810	434,067/861,635
Valid	3,524/3,704	2,145/2,184	3,520/3,599	3,451/6,955
Test	1,144/1,189	543/552	1,300/1,310	973/1,870
Total	446,139/471,618	275,011/279,985	445,934/453,719	438,491/870,460

Table 3. Distribution statistics of question types (T) and number of bounding boxes (B) across data splits.

proximately 1.6 million VQA pairs. The reports containing less than two sentences will not be used to generate QAs. The detailed prompt is elaborated in Table 2. At this point, the generated visual location is still the anatomical region in text format (e.g., “left lower lung zone”). In order for the further VQA model to ground the specific location on the image, we need to perform a post-processing step to map the region to bounding box coordinates. An example demonstrating multi-modal explainability is presented in Figure 2, with further cases available in the Appendix.

**Dataset Split.** Our generated VQAs are partitioned in accordance with the MIMIC-CXR distribution. Specifically, we have 149,535 images with 1,588,975 QA pairs for training, 1,190 images with 12,640 QA pairs for validation, and 300 images with 3,960 QA pairs for testing. It is important to note that the test set is manually cleaned according to involved diseases [19] from the original one (about 2,331 images), serving as a gold standard for evaluating the quality of the automatically generated VQAs and for benchmarking the large vision language models. Detailed statistics, including question type distribution and the number of bounding boxes, are shown in Table 3. More

data, such as word cloud and common chest disease statistics, are provided in the Appendix.

## 4. Evaluation of GEMeX

### 4.1. Experimental Details

**A Strong Baseline Fine-Tuned on GEMeX.** To validate the effectiveness of the dataset, especially the auto-generated training set, we propose a question-type-aware instruction tuning to fine-tune LLaVA-Med-v1-7B [26] on the training set of GEMeX, termed as LLaVA-Med-GEMeX, serving as a simple baseline. Specifically, for each VQA sample from our GEMeX, we add a type prompt  $X_{Type}$  after the original system prompt and a question  $X_{Question}$  with its answer  $X_{Answer}$ , textual reason  $X_{Reason}$ , and corresponding visual location  $X_{Location}$ , constructing a single-turn dialogue as in Table 4. Generally,  $X_{Type}$  is “Input an {Type} question, and the assistant will output its answer {Supplement} with a detailed reason and corresponding visual location.” where {Type} refers to “open-ended/closed-ended/single-choice/multi-choice” and {Supplement} is replaced by “none/(yes or no)/(an option)/(some options)”, respectively. We have shown some input samples in the Appendix.

```
<Ori_System_Prompt>  $X_{Type}$  <STOP>
Human: <image>\n $X_{Question}$   $X_{Choices}$  (if any)
<STOP>
Assistant: <answer> $X_{Answer}$  <reason> $X_{Reason}$ 
<location> $X_{Location}$  <STOP>
```

Table 4. Input format for fine-tuning LLaVA-Med.

Models	Open-ended		Closed-ended			Single-choice			Multi-choice			Avg. †
	AR-score †	V-score	A-score	AR-score †	V-score	A-score	AR-score †	V-score	A-score	AR-score †	V-score	
Random	-	-	48.80	-	-	25.85	-	-	7.50	-	-	-
GPT-4o-mini [1]	<b>97.68</b>	<u>18.05</u>	59.30	71.14	<u>28.64</u>	<u>59.00</u>	<u>77.47</u>	<u>23.62</u>	<u>49.13</u>	<u>82.91</u>	<u>19.19</u>	<u>82.30</u>
LLaVA-v1 [35]	76.14	-	30.76	38.02	-	-	50.47	-	-	66.52	-	57.79
LLaVA-v1.5 [34]	77.62	-	58.93	57.00	-	47.00	57.05	-	-	65.17	-	64.21
Mini-GPT4-v1 [57]	55.32	-	26.33	31.09	-	-	37.63	-	-	46.65	-	42.67
mPLUG-Owl [48]	76.73	-	27.26	36.70	-	32.00	46.89	-	-	67.92	-	57.06
LLaVA-Med-v1 [26]	90.34	-	62.62	69.91	-	-	61.74	-	-	68.14	-	72.53
LLaVA-Med-v1.5 [26]	94.43	-	<u>71.82</u>	<u>76.54</u>	-	-	66.04	-	-	67.28	-	76.07
MiniGPT-Med [3]	86.12	-	55.24	65.25	-	-	55.61	-	-	64.33	-	67.83
XrayGPT [40]	81.17	-	-	68.17	-	-	48.33	-	-	55.10	-	63.19
RadFM [43]	88.57	-	58.01	67.91	-	-	57.82	-	-	62.41	-	69.18
<b>LLaVA-Med-GEMeX</b>	<u>97.05</u>	<b>51.47</b>	<b>77.35</b>	<b>80.72</b>	<b>53.20</b>	<b>73.08</b>	<b>81.42</b>	<b>54.57</b>	<b>67.42</b>	<b>84.98</b>	<b>47.99</b>	<b>86.04</b>

Table 5. Performance of representative LVLMs on our GEMeX across four different question types. The AR-score combines answer and reasoning to evaluate textual output performance. † denotes the GPTScore value (%). The A-score indicates answer or choice accuracy (%), and the V-score represents mIoU (%). The best results are bolded, and the second-best are underlined in each column.

**Training Details.** We fine-tune both the visual projection layers and the LLM components of LLaVA-Med-v1 (after stage II) by calculating the auto-regressive loss to predict the assistant’s responses and the dialogue termination token <STOP>. Particularly, the model is trained for 3 epochs on four NVIDIA H100 GPUs with a batch size of 64, taking around 54 hours. The network is warmed up in the first 0.03 epochs with a linear learning rate from 3e-7 to 2e-5, which further decays by cosine schedule. The optimizer is AdamW. To accelerate training, we employ the Fully Sharded Data Parallel (FSDP) mechanism, the bf16 (Brain Floating Point) data format, and gradient checkpointing.

**LVLMs Benchmarks.** Besides fine-tuning a task-oriented model, we perform a zero-shot evaluation on our GEMeX dataset across the other 10 LVLMs, with 5 in the general domain and the other 5 in the medical domain:

- **In the General Domain:** we test LLaVA-v1 [35], Mini-GPT4-v1 [57], mPLUG-Owl [48], LLaVA-v1.5 [34], and GPT-4o-mini. Note that we did not test GPT-4o because its safety protection policy prohibits it from analyzing medical images.
- **In the Medical Domain:** we evaluate LLaVA-Med-v1 [26], LLaVA-Med-v1.5 [26], MiniGPT-Med [3], XrayGPT [40], and RadFM [43]. A detailed introduction can be found in the Appendix.

## 4.2. Evaluation Metrics

In GEMeX, each question has a corresponding answer, textual reason, and visual location. Ideally, we aim to evaluate all these three aspects with designed metrics as follows:

- **Answer-Reason Score (AR-score):** In reality, most LVLMs struggle to generate accurate outputs in terms of format. This doesn’t necessarily mean these models lack the knowledge to answer the questions but rather simply

lack the ability to follow instructions properly. To ensure a fair comparison, we introduce the Answer-Reason score (AR-score) as an evaluation metric for the textual output, where the answer and reason parts from each test sample are merged as a reference (ground truth), and the evaluated LVLM’s output serve as a candidate. We use GPTScore [26] to calculate the AR-Score from a semantic perspective. Specifically, GPT-4o is leveraged to quantify the correctness. We start by treating the aforementioned reference as a textual response from assistant #1, while the candidate as the response from assistant #2. With both responses, the original question, and the X-ray report, GPT-4o assesses the accuracy, relevance, and helpfulness of each assistant’s answer and provides an overall score on a scale of 1 to 10, where a higher score indicates better performance. We then calculate the relative score using GPT-4o’s reference score for normalization. Besides, we also employ common NLG metrics (e.g., BERTScore [52], BLEU, ROUGE) to evaluate AR-score.

- **Answer Score (A-score):** For responses where the model can output specific answers (such as yes/no for closed-ended questions or options for single/multiple choice questions), we calculate the accuracy by comparing with the ground truth. It is worth noting that although some models cannot directly output the answer, we still attempt to match it from their responses.
- **Visual Score (V-score):** For models capable of visual grounding (i.e., outputting visual locations), we calculated mean intersection over union (mIoU) as a measurement. For a VQA case, considering there might be multiple corresponding locations (commonly seen in multiple-choice questions), we use the Hungarian algorithm [23] to match the predicted bounding boxes with the actual ones.

Models	Open-ended			Closed-ended			Single-choice			Multi-choice		
	BERTScore	ROUGE-L	BLEU-1	BERTScore	ROUGE-L	BLEU-1	BERTScore	ROUGE-L	BLEU-1	BERTScore	ROUGE-L	BLEU-1
GPT-4o-mini [1]	<u>30.43</u>	<u>22.67</u>	<u>18.25</u>	40.02	25.63	19.10	<u>48.34</u>	<u>39.17</u>	<u>30.82</u>	<u>46.58</u>	<u>39.20</u>	<u>28.65</u>
LLaVA-v1 [35]	20.09	15.22	11.57	22.42	13.10	8.01	20.25	14.97	10.61	19.69	17.35	11.15
LLaVA-v1.5 [34]	21.49	16.11	12.20	32.59	15.37	6.69	17.42	17.53	1.49	23.74	21.20	8.95
Mini-GPT4-v1 [57]	15.03	14.66	11.46	13.83	9.65	6.31	6.50	6.79	4.60	5.31	5.79	3.22
mPLUG-Owl [48]	22.52	17.03	13.22	<b>32.23</b>	20.20	13.92	39.64	33.69	30.32	26.09	24.97	16.68
LLaVA-Med-v1 [26]	25.14	19.63	15.93	38.04	29.08	19.74	34.89	30.10	25.84	28.63	26.51	20.99
LLaVA-Med-v1.5 [26]	26.42	21.38	17.28	<u>44.48</u>	<u>36.73</u>	<u>26.35</u>	36.62	30.32	25.44	28.11	24.49	16.53
MiniGPT-Med [3]	23.47	19.20	16.03	34.31	29.47	19.13	30.11	28.51	22.13	26.51	24.42	15.98
XrayGPT [40]	22.57	18.30	15.73	21.35	14.55	10.17	16.31	12.17	9.23	12.15	10.30	6.22
RadFM [43]	24.96	20.71	17.73	37.43	27.95	20.56	32.30	27.02	24.39	25.81	20.02	13.80
<b>LLaVA-Med-GEMeX</b>	<b>42.69</b>	<b>32.75</b>	<b>25.28</b>	<b>54.44</b>	<b>38.39</b>	<b>33.99</b>	<b>56.35</b>	<b>53.23</b>	<b>47.31</b>	<b>54.95</b>	<b>50.85</b>	<b>43.99</b>

Table 6. Performance of representative LVLMS evaluated using various natural language generation metrics for AR-score, including BERTScore, ROUGE-L, and BLEU-1. The best results are bolded, and the second-best are underlined in each column.

### 4.3. Results and Analysis

**Overall Performance.** To make a fair comparison, the evaluated models (except GPT-4o-mini and RadFM (with MedLLaMA-13B [44])) are based on 7B-LLMs in this section. Specifically, LLaVA-v1, LLaVA-Med-v1, and Mini-GPT4-v1 are based on Vicuna-v0-7B [10] while LLaVA-v1.5 and XrayGPT are based on Vicuna-v1-7B; LLaVA-Med-v1.5 is built upon Mistral-7B-Instruct-v0.2 [20]; mPLUG-Owl is using LLaMA-7B [41]. All models’ configurations are set according to their open-source codes. The comprehensive results are shown in Table 5. The first 5 rows indicate the performance of general LVLMS, while the last 6 rows present the results of medical ones and our fine-tuned version of LLaVA-Med-v1 (termed as LLaVA-Med-GEMeX). It can be found that:

- **Most available LVLMS exhibit weak performance when tested on GEMeX.** The only exception is GPT-4o-mini, which achieves an AR-score above 80 on average across all tasks. When considering specific question types, LLaVA-Med (both versions 1 and 1.5) stands out for its strong performance on open-ended questions, scoring above 90 on the AR-score. However, all models show poor results on the other three categories of tasks.
- **When faced with choice-based questions, most models struggle to output definitive options,** although they can analyze each option. This explains why most models have a corresponding AR-score but lack an A-score, demonstrating the need of introducing these types of questions.
- **Powerful LVLMS like GPT-4o-mini often rely on shortcut reasoning instead of true multimodal reasoning.** Specifically, while they can sometimes answer questions to a certain extent, they often fail to accurately visual grounding. This indicates that these models tend to solve Med-VQA tasks using shortcut knowledge, such as retrieving information from their pre-training memory, rather than engaging in genuine multimodal reasoning. However, multimodal reasoning is central to the explain-

ability of Med-VQA systems.

- Through the proposed simple question-type-aware instruction tuning, the model achieves a significant performance improvement, approximately **13.5%** (*i.e.*, avg. AR-score) compared to LLaVA-Med-v1. More importantly, it surpasses GPT-4o-mini on most metrics, demonstrating the reliability of the training set. However, there still remains a significant gap towards practical usage, highlighting the challenges of the proposed GEMeX.

**Limitation.** We want to emphasize that the fine-tuned model is inherently task-specific, which means it may suffer from reduced accuracy on other datasets or lose its ability to engage in conversations. Therefore, the real potential lies in integrating our GEMeX into multi-task training (such as the second stage of training LLaVA-Med) in the future. The tuned model here primarily serves to validate the effectiveness of the dataset while also establishing a robust baseline.

**More Metrics.** As we mentioned in Section 4.2, we also calculate NLG metrics to measure AR-score. Detailed results are shown in Table 6. Overall, the NLG metrics generally share the same trend as GPTScore (AR-score in Table 5), but there are some minor differences. (1) Models with high NLG scores do not always correlate with good performance, as seen with mPLUG-Owl compared to LLaVA-v1.5. Essentially, LLaVA-1.5 demonstrates higher performance, such as achieving an answer accuracy rate (A-score) in single-choice tasks that is **15%** higher than that of mPLUG-Owl. However, since LLaVA-v1.5’s output mostly consists of the answer without reason, the shorter output results in a lower NLG score, with its BLEU-1 approximately **28.8%** lower than mPLUG-Owl; (2) NLG metrics can better reflect the performance improvement after fine-tuning. For example, the fine-tuned model shows only about a 3.7% average improvement over GPT-4o-mini on GPTScore but brings around a **12.1%** improvement on average NLG metrics. This more significant improvement bet-

Challenging examples from GEMeX:

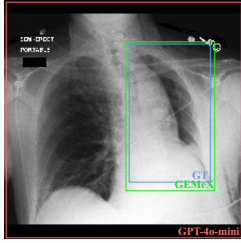
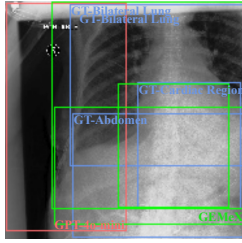
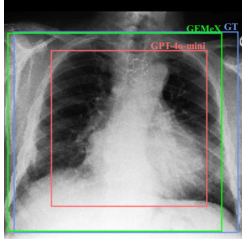
	CASE I	CASE II	CASE III
			
	(Bbox predicted by each model)	(Bbox predicted by each model)	(Bbox predicted by each model)
<i>Question</i>	What might be the cause of the overexpansion of the right lung?	What regions on the X-ray indicate abnormal findings? Choices: [A: Bilateral lung, B: Cardiac region, C: Abdomen, D: Spine]	What is the overall condition of the lungs based on the CXR? Choices: [A: Clear, B: Consolidated, C: Effused, D: Thickened]
<i>Ground Truth</i>	<Answer>: Compensatory hyperinflation due to left lung removal. <Reason>: After a pneumonectomy, the remaining lung may overexpand to compensate for the <b>loss of the left lung</b> .	<Answer>: [A, B, C]. <Reason>: <b>The bilateral lung shows pleural effusion</b> , the cardiac region shows enlargement, and <b>the abdomen shows the nasogastric tube</b> . The spine is normal.	<Answer>: A. <Reason>: The CXR indicates that <b>the lungs are clear of consolidation or effusion</b> , although <b>right pleural-based thickening at the base</b> .
GPT-4o-mini	<Answer>: The overexpansion of the right lung may be caused by conditions such as a right-sided pneumothorax or chronic obstructive pulmonary disease (COPD). <Reason>: Overexpansion can occur when air enters the pleural space (as in pneumothorax) or when there is an obstruction that prevents air from leaving the lung, causing it to become hyperinflated. In COPD, the lung tissue loses elasticity, leading to overinflation. <GPTScore>: 44.44	<Answer>: [A: Bilateral lung]. <Reason>: <b>The bilateral lung region shows potential abnormalities such as opacities or other irregularities that may indicate pathology (✗)</b> . <GPTScore>: 37.50	<Answer>: B. <Reason>: <b>The presence of increased opacity in the lung fields suggests consolidation</b> , indicating that the lungs are not clear and may have fluid or solid material in the alveoli (✗). <GPTScore>: 33.33.
LLaVA-Med-GEMeX	<Answer>: Possible chronic lung disease or compensatory mechanism (✓). <Reason>: Overexpansion of the lung can be due to chronic lung diseases or compensatory mechanisms, especially <b>after a left lobectomy (✓)</b> . <GPTScore>: 66.67	<Answer>: [A, B, C]. <Reason>: <b>The bilateral lung shows interstitial opacities (✗)</b> , the cardiac region shows enlargement (✓), and <b>the abdomen shows the feeding tube location (✓)</b> . <GPTScore>: 87.50	<Answer>: A. <Reason>: The CXR indicates that <b>the lungs are otherwise clear except for the noted pleural thickening (✓)</b> . <GPTScore>: 88.89

Table 7. Challenging questions from GEMeX answered by GPT-4o-mini and our fine-tuned LLaVA-Med-GEMeX. These examples highlight the limitations of LVLMS like GPT-4o-mini in visual reasoning, which can be effectively improved by fine-tuning with GEMeX.

ter demonstrates the model’s learning effect on the dataset. Overall, we believe that for models that have not participated in GEMeX training, using GPTScore is more reasonable, as semantic understanding can be used to judge the difference between the model’s output and the true label. For fine-tuned models, NLG metrics are preferred because they can better reflect the model’s alignment with the dataset.

**Case Study.** In Table 7, we show some questions with outputs from both GPT-4o-mini and our fine-tuned LLaVA-Med-GEMeX for qualitative comparison. In CASE I, although GPT-4o-mini can generate a very detailed answer, it provides answers without reasoning on the visual content, resulting in a significant difference from the ground truth. In contrast, the LLaVA-Med-GEMeX offers relatively accurate visual clues and is able to provide partially correct answers (“the compensatory mechanism”), although there is a false mention of “possible chronic lung disease” when considering the patient’s condition. In CASE II, although GPT-4o-mini can analyze images, its limited capabilities result in selecting only one option and providing a vague reason. In contrast, the LLaVA-Med-GEMeX outputs the correct options but gives an incorrect reason for one op-

tion (*i.e.*, answer “A”). In CASE III, GPT-4o-mini cannot both visually reason and output answers correctly, while the fine-tuned model can give better outputs from these two aspects. From these examples, we can conclude that some LVLMS still lack sufficient understanding of medical images. Meanwhile, while the proposed simple fine-tuning method improves performance, it is still far from fully accurate, leaving much room for further exploration. We have provided more case studies in the Appendix.

## 5. Conclusion

In this paper, we introduce a benchmark, GEMeX, designed to advance the field of medical VQA with two primary advantages: multimodal explainability and diverse question types. GEMeX not only provides more accessible medical explanations for patients and junior doctors but also serves as a valuable training resource for developing next-generation medical LVLMS with enhanced instruction-following capabilities. We demonstrate the effectiveness and difficulty of the dataset through comprehensive testing of representative LVLMS as well as task-specific fine-tuning, hoping that GEMeX can promote medical VQA development and improve AI-assisted medical care.



## References

- [1] Josh Achiam, Steven Adler, Sandhini Agarwal, Lama Ahmad, Ilge Akkaya, Florencia Leoni Aleman, Diogo Almeida, Janko Altenschmidt, Sam Altman, Shyamal Anadkat, et al. Gpt-4 technical report. *arXiv preprint arXiv:2303.08774*, 2023. 1, 2, 4, 6, 7
- [2] Jean-Baptiste Alayrac, Jeff Donahue, Pauline Luc, Antoine Miech, Iain Barr, Yana Hasson, Karel Lenc, Arthur Mensch, Katherine Millican, Malcolm Reynolds, et al. Flamingo: a visual language model for few-shot learning. *Advances in neural information processing systems*, 35:23716–23736, 2022. 1
- [3] Asma Alkhalidi, Raneem Alnajim, Layan Alabdullatef, Rawan Alyahya, Jun Chen, Deyao Zhu, Ahmed Alsinan, and Mohamed Elhoseiny. Minigpt-med: Large language model as a general interface for radiology diagnosis. *arXiv preprint arXiv:2407.04106*, 2024. 3, 6, 7, 4
- [4] Seongsu Bae, Daeun Kyung, Jaehyeon Ryu, Eunbyeol Cho, Gyubok Lee, Sunjun Kwon, Jungwoo Oh, Lei Ji, Eric Chang, Tackeun Kim, et al. Ehrxqa: A multi-modal question answering dataset for electronic health records with chest x-ray images. *Advances in Neural Information Processing Systems*, 36, 2024. 2, 3, 4
- [5] Jinze Bai, Shuai Bai, Shusheng Yang, Shijie Wang, Sinan Tan, Peng Wang, Junyang Lin, Chang Zhou, and Jingren Zhou. Qwen-vl: A versatile vision-language model for understanding, localization, text reading, and beyond. *arXiv preprint arXiv:2308.12966*, 1(2):3, 2023. 1
- [6] Asma Ben Abacha, Mourad Sarrouiti, Dina Demner-Fushman, Sadid A Hasan, and Henning Müller. Overview of the vqa-med task at imageclef 2021: Visual question answering and generation in the medical domain. In *Proceedings of the CLEF 2021 Conference and Labs of the Evaluation Forum-working notes*. 21-24 September 2021, 2021. 2, 3
- [7] Xiaolan Chen, Ziwei Zhao, Weiyi Zhang, Pusheng Xu, Le Gao, Mingpu Xu, Yue Wu, Yinwen Li, Danli Shi, and Mingguang He. Eyegpt: Ophthalmic assistant with large language models. *arXiv preprint arXiv:2403.00840*, 2024. 3
- [8] Zhihong Chen, Yuhao Du, Jinpeng Hu, Yang Liu, Guanbin Li, Xiang Wan, and Tsung-Hui Chang. Multi-modal masked autoencoders for medical vision-and-language pre-training. In *International Conference on Medical Image Computing and Computer-Assisted Intervention*, pages 679–689. Springer, 2022. 3
- [9] Zhihong Chen, Shizhe Diao, Benyou Wang, Guanbin Li, and Xiang Wan. Towards unifying medical vision-and-language pre-training via soft prompts. In *Proceedings of the IEEE/CVF International Conference on Computer Vision*, pages 23403–23413, 2023. 3
- [10] Wei-Lin Chiang, Zhuohan Li, Zi Lin, Ying Sheng, Zhanghao Wu, Hao Zhang, Lianmin Zheng, Siyuan Zhuang, Yonghao Zhuang, Joseph E Gonzalez, et al. Vicuna: An open-source chatbot impressing gpt-4 with 90%\* chatgpt quality. See <https://vicuna.lmsys.org> (accessed 14 April 2023), 2(3):6, 2023. 7
- [11] Wenliang Dai, Junnan Li, Dongxu Li, Anthony Meng Huat Tiong, Junqi Zhao, Weisheng Wang, Boyang Li, Pascale Fung, and Steven Hoi. Instructblip: Towards general-purpose vision-language models with instruction tuning, 2023. 1
- [12] Sedigheh Eslami, Gerard de Melo, and Christoph Meinel. Does clip benefit visual question answering in the medical domain as much as it does in the general domain? *arXiv preprint arXiv:2112.13906*, 2021. 3
- [13] Yujie Feng, Zexin Lu, Bo Liu, Liming Zhan, and Xiaoming Wu. Towards llm-driven dialogue state tracking. *arXiv preprint arXiv:2310.14970*, 2023. 1
- [14] Haifan Gong, Guanqi Chen, Sishuo Liu, Yizhou Yu, and Guanbin Li. Cross-modal self-attention with multi-task pre-training for medical visual question answering. In *Proceedings of the 2021 international conference on multimedia retrieval*, pages 456–460, 2021. 3
- [15] Zhaopeng Gu, Bingke Zhu, Guibo Zhu, Yingying Chen, Ming Tang, and Jinqiao Wang. Anomalygpt: Detecting industrial anomalies using large vision-language models. In *Proceedings of the AAAI Conference on Artificial Intelligence*, pages 1932–1940, 2024. 1
- [16] Xuehai He, Yichen Zhang, Luntian Mou, Eric Xing, and Pengtao Xie. Pathvqa: 30000+ questions for medical visual question answering. *arXiv preprint arXiv:2003.10286*, 2020. 1, 2, 3
- [17] Xinyue Hu, Lin Gu, Qiyuan An, Mengliang Zhang, Liangchen Liu, Kazuma Kobayashi, Tatsuya Harada, Ronald M Summers, and Yingying Zhu. Expert knowledge-aware image difference graph representation learning for difference-aware medical visual question answering. In *Proceedings of the 29th ACM SIGKDD Conference on Knowledge Discovery and Data Mining*, pages 4156–4165, 2023. 2, 3, 4
- [18] Yutao Hu, Tianbin Li, Quanfeng Lu, Wenqi Shao, Junjun He, Yu Qiao, and Ping Luo. Omnimedvqa: A new large-scale comprehensive evaluation benchmark for medical lvlm. In *Proceedings of the IEEE/CVF Conference on Computer Vision and Pattern Recognition*, pages 22170–22183, 2024. 1, 2, 3
- [19] Jeremy Irvin, Pranav Rajpurkar, Michael Ko, Yifan Yu, Silvana Ciurea-Ilcus, Chris Chute, Henrik Marklund, Behzad Haghgoo, Robyn Ball, Katie Shpanskaya, et al. Chexpert: A large chest radiograph dataset with uncertainty labels and expert comparison. In *Proceedings of the AAAI conference on artificial intelligence*, pages 590–597, 2019. 5, 4
- [20] Albert Q Jiang, Alexandre Sablayrolles, Arthur Mensch, Chris Bamford, Devendra Singh Chaplot, Diego de las Casas, Florian Bressand, Gianna Lengyel, Guillaume Lample, Lucile Saulnier, et al. Mistral 7b. *arXiv preprint arXiv:2310.06825*, 2023. 7
- [21] Alistair EW Johnson, Tom J Pollard, Seth J Berkowitz, Nathaniel R Greenbaum, Matthew P Lungren, Chih-ying Deng, Roger G Mark, and Steven Horng. Mimic-cxr, a de-identified publicly available database of chest radiographs with free-text reports. *Scientific data*, 6(1):317, 2019. 3
- [22] Yash Khare, Viraj Bagal, Minesh Mathew, Adithi Devi, U Deva Priyakumar, and CV Jawahar. Mmbert: Multi-modal bert pretraining for improved medical vqa. In *2021*

- IEEE 18th International Symposium on Biomedical Imaging (ISBI)*, pages 1033–1036. IEEE, 2021. 3
- [23] Harold W Kuhn. The hungarian method for the assignment problem. *Naval research logistics quarterly*, 2(1-2):83–97, 1955. 6
- [24] Jason J Lau, Soumya Gayen, Asma Ben Abacha, and Dina Demner-Fushman. A dataset of clinically generated visual questions and answers about radiology images. *Scientific data*, 5(1):1–10, 2018. 1, 2, 3
- [25] Suhyeon Lee, Won Jun Kim, Jinho Chang, and Jong Chul Ye. Llm-cxr: Instruction-finetuned llm for cxr image understanding and generation. *arXiv preprint arXiv:2305.11490*, 2023. 3
- [26] Chunyuan Li, Cliff Wong, Sheng Zhang, Naoto Usuyama, Haotian Liu, Jianwei Yang, Tristan Naumann, Hoifung Poon, and Jianfeng Gao. Llava-med: Training a large language-and-vision assistant for biomedicine in one day. *Advances in Neural Information Processing Systems*, 36, 2024. 2, 3, 5, 6, 7, 4
- [27] Qing Li, Qingyi Tao, Shafiq Joty, Jianfei Cai, and Jiebo Luo. Vqa-e: Explaining, elaborating, and enhancing your answers for visual questions. In *Proceedings of the European Conference on Computer Vision (ECCV)*, pages 552–567, 2018. 1
- [28] Weixiong Lin, Ziheng Zhao, Xiaoman Zhang, Chaoyi Wu, Ya Zhang, Yanfeng Wang, and Weidi Xie. Pmc-clip: Contrastive language-image pre-training using biomedical documents. In *International Conference on Medical Image Computing and Computer-Assisted Intervention*, pages 525–536. Springer, 2023. 3
- [29] Zhihong Lin, Donghao Zhang, Qingyi Tao, Danli Shi, Gholamreza Haffari, Qi Wu, Mingguang He, and Zongyuan Ge. Medical visual question answering: A survey. *Artificial Intelligence in Medicine*, 143:102611, 2023. 1
- [30] Bo Liu, Li-Ming Zhan, and Xiao-Ming Wu. Contrastive pre-training and representation distillation for medical visual question answering based on radiology images. In *Medical Image Computing and Computer Assisted Intervention—MICCAI 2021: 24th International Conference, Strasbourg, France, September 27–October 1, 2021, Proceedings, Part II 24*, pages 210–220. Springer, 2021. 3
- [31] Bo Liu, Li-Ming Zhan, Li Xu, Lin Ma, Yan Yang, and Xiao-Ming Wu. Slake: A semantically-labeled knowledge-enhanced dataset for medical visual question answering. In *2021 IEEE 18th International Symposium on Biomedical Imaging (ISBI)*, pages 1650–1654. IEEE, 2021. 1, 2
- [32] Bo Liu, Li-Ming Zhan, Li Xu, and Xiao-Ming Wu. Medical visual question answering via conditional reasoning and contrastive learning. *IEEE transactions on medical imaging*, 42(5):1532–1545, 2022. 3
- [33] Fenglin Liu, Shen Ge, Yuexian Zou, and Xian Wu. Competence-based multimodal curriculum learning for medical report generation. *arXiv preprint arXiv:2206.14579*, 2022. 4
- [34] Haotian Liu, Chunyuan Li, Yuheng Li, and Yong Jae Lee. Improved baselines with visual instruction tuning. In *Proceedings of the IEEE/CVF Conference on Computer Vision and Pattern Recognition*, pages 26296–26306, 2024. 6, 7, 4
- [35] Haotian Liu, Chunyuan Li, Qingyang Wu, and Yong Jae Lee. Visual instruction tuning. *Advances in neural information processing systems*, 36, 2024. 1, 2, 3, 6, 7, 4
- [36] Jong Hak Moon, Hyungyung Lee, Woncheol Shin, Young-Hak Kim, and Edward Choi. Multi-modal understanding and generation for medical images and text via vision-language pre-training. *IEEE Journal of Biomedical and Health Informatics*, 26(12):6070–6080, 2022. 3
- [37] Alec Radford, Jong Wook Kim, Chris Hallacy, Aditya Ramesh, Gabriel Goh, Sandhini Agarwal, Girish Sastry, Amanda Askell, Pamela Mishkin, Jack Clark, et al. Learning transferable visual models from natural language supervision. In *International conference on machine learning*, pages 8748–8763. PMLR, 2021. 3
- [38] Aditya Ramesh, Mikhail Pavlov, Gabriel Goh, Scott Gray, Chelsea Voss, Alec Radford, Mark Chen, and Ilya Sutskever. Zero-shot text-to-image generation. In *International conference on machine learning*, pages 8821–8831. Pmlr, 2021. 1
- [39] Tim Tanida, Philip Müller, Georgios Kaissis, and Daniel Rueckert. Interactive and explainable region-guided radiology report generation. In *Proceedings of the IEEE/CVF Conference on Computer Vision and Pattern Recognition*, pages 7433–7442, 2023. 4
- [40] Omkar Thawkar, Abdelrahman Shaker, Sahal Shaji Mullappilly, Hisham Cholakkal, Rao Muhammad Anwer, Salman Khan, Jorma Laaksonen, and Fahad Shahbaz Khan. Xraygpt: Chest radiographs summarization using medical vision-language models. *arXiv preprint arXiv:2306.07971*, 2023. 2, 3, 6, 7, 4
- [41] Hugo Touvron, Thibaut Lavril, Gautier Izacard, Xavier Martinet, Marie-Anne Lachaux, Timothée Lacroix, Baptiste Rozière, Naman Goyal, Eric Hambro, Faisal Azhar, et al. Llama: Open and efficient foundation language models. *arXiv preprint arXiv:2302.13971*, 2023. 7
- [42] Xiyue Wang, Junhan Zhao, Eliana Marostica, Wei Yuan, Jietian Jin, Jiayu Zhang, Ruijiang Li, Hongping Tang, Kanran Wang, Yu Li, et al. A pathology foundation model for cancer diagnosis and prognosis prediction. *Nature*, pages 1–9, 2024. 3
- [43] Chaoyi Wu, Xiaoman Zhang, Ya Zhang, Yanfeng Wang, and Weidi Xie. Towards generalist foundation model for radiology. *arXiv preprint arXiv:2308.02463*, 2023. 2, 3, 6, 7, 4
- [44] Chaoyi Wu, Weixiong Lin, Xiaoman Zhang, Ya Zhang, Weidi Xie, and Yanfeng Wang. Pmc-llama: toward building open-source language models for medicine. *Journal of the American Medical Informatics Association*, page ocae045, 2024. 7
- [45] Joy T Wu, Nkechinyere N Agu, Ismini Lourentzou, Arjun Sharma, Joseph A Paguio, Jasper S Yao, Edward C Dee, William Mitchell, Satyananda Kashyap, Andrea Giovannini, et al. Chest imagenome dataset for clinical reasoning. *arXiv preprint arXiv:2108.00316*, 2021. 2, 4
- [46] Li Xu, Bo Liu, Ameer Hamza Khan, Lu Fan, and Xiao-Ming Wu. Multi-modal pre-training for medical vision-language understanding and generation: An empirical study with a new benchmark. *arXiv preprint arXiv:2306.06494*, 2023. 3

- [47] Peng Xu, Wenqi Shao, Kaipeng Zhang, Peng Gao, Shuo Liu, Meng Lei, Fanqing Meng, Siyuan Huang, Yu Qiao, and Ping Luo. Lvlm-ehub: A comprehensive evaluation benchmark for large vision-language models. *arXiv preprint arXiv:2306.09265*, 2023. 1
- [48] Qinghao Ye, Haiyang Xu, Guohai Xu, Jiabo Ye, Ming Yan, Yiyang Zhou, Junyang Wang, Anwen Hu, Pengcheng Shi, Yaya Shi, et al. mplug-owl: Modularization empowers large language models with multimodality. *arXiv preprint arXiv:2304.14178*, 2023. 6, 7, 4
- [49] Kihyun You, Jawook Gu, Jiyeon Ham, Beomhee Park, Jiho Kim, Eun K Hong, Woonhyuk Baek, and Byungseok Roh. Cxr-clip: Toward large scale chest x-ray language-image pre-training. In *International Conference on Medical Image Computing and Computer-Assisted Intervention*, pages 101–111. Springer, 2023. 3
- [50] Li-Ming Zhan, Bo Liu, Lu Fan, Jiaxin Chen, and Xiao-Ming Wu. Medical visual question answering via conditional reasoning. In *Proceedings of the 28th ACM International Conference on Multimedia*, pages 2345–2354, 2020. 3
- [51] Sheng Zhang, Yanbo Xu, Naoto Usuyama, Hanwen Xu, Jaspreet Bagga, Robert Tinn, Sam Preston, Rajesh Rao, Mu Wei, Naveen Valluri, et al. Biomedclip: a multimodal biomedical foundation model pretrained from fifteen million scientific image-text pairs. *arXiv preprint arXiv:2303.00915*, 2023. 3
- [52] Tianyi Zhang, Varsha Kishore, Felix Wu, Kilian Q Weinberger, and Yoav Artzi. Bertscore: Evaluating text generation with bert. *arXiv preprint arXiv:1904.09675*, 2019. 6
- [53] Xiaoman Zhang, Chaoyi Wu, Ziheng Zhao, Weixiong Lin, Ya Zhang, Yanfeng Wang, and Weidi Xie. Pmc-vqa: Visual instruction tuning for medical visual question answering. *arXiv preprint arXiv:2305.10415*, 2023. 1, 2, 3
- [54] Xiaoman Zhang, Chaoyi Wu, Ziheng Zhao, Jiayu Lei, Ya Zhang, Yanfeng Wang, and Weidi Xie. Radgenome-chest ct: A grounded vision-language dataset for chest ct analysis. *arXiv preprint arXiv:2404.16754*, 2024. 2, 3
- [55] Xiangyu Zhao, Bo Liu, Qijiong Liu, Guangyuan Shi, and Xiao-Ming Wu. Easygen: Easing multimodal generation with bidiffuser and llms. In *Proceedings of the 62nd Annual Meeting of the Association for Computational Linguistics (Volume 1: Long Papers)*, pages 1351–1370, 2024. 1
- [56] Juexiao Zhou, Xiaonan He, Liyuan Sun, Jiannan Xu, Xiuying Chen, Yuetan Chu, Longxi Zhou, Xingyu Liao, Bin Zhang, and Xin Gao. Skingpt-4: an interactive dermatology diagnostic system with visual large language model. *arXiv preprint arXiv:2304.10691*, 2023. 3
- [57] Deyao Zhu, Jun Chen, Xiaoqian Shen, Xiang Li, and Mohamed Elhoseiny. Minigpt-4: Enhancing vision-language understanding with advanced large language models. *arXiv preprint arXiv:2304.10592*, 2023. 1, 2, 6, 7, 4
- [58] Ke Zou, Yang Bai, Zhihao Chen, Yang Zhou, Yidi Chen, Kai Ren, Meng Wang, Xuedong Yuan, Xiaojing Shen, and Huazhu Fu. Medrg: Medical report grounding with multi-modal large language model. *arXiv preprint arXiv:2404.06798*, 2024. 3

# GEMeX: A Large-Scale, Groundable, and Explainable Medical VQA Benchmark for Chest X-ray Diagnosis

## Supplementary Material

	Chest ImaGenome	Ours
Reserve	right lung, right mid lung zone, right hilar structures, right hemidiaphragm, left lung, left mid lung zone, left hilar structures, left hemidiaphragm, trachea, spine, abdomen, svc	right lung, right mid lung zone, right hilar structures, right hemidiaphragm, left lung, left mid lung zone, left hilar structures, left hemidiaphragm, trachea, spine, abdomen, svc
Incorporate	left upper lung zone left apical zone	left upper lung zone
	right upper lung zone right apical zone	right upper lung zone
	mediastinum upper mediastinum	mediastinum
	right lower lung zone right costophrenic angle	right lower lung zone
	left lower lung zone left costophrenic angle	left lower lung zone
	cardiac silhouette cavoatrial junction right atrium	cardiac silhouette
Delete	carina right clavicle left clavicle aortic arch	-
	left lung + right lung	bilateral lung
	left upper + right upper	bilateral upper lung zone
	left mid + right mid	bilateral mid lung zone
Merge	left lower + right lower	bilateral lower lung zone
	left hilar + right hilar	bilateral hilar structures
	left hemidiaphragm + right hemidiaphragm	bilateral hemidiaphragm
	left mid + left lower	left mid-to-lower lung zone
	right mid + right lower	right mid-to-lower lung zone
	left mid + left upper	left mid-to-upper lung zone
	right mid + right upper	right mid-to-upper lung zone
	left mid-to-lower + right mid-to-lower	bilateral mid-to-lower lung zone
	left mid-to-upper + right mid-to-upper	bilateral mid-to-upper lung zone
	Sum	29

Table 8. Anatomical regions transformation from the Chest ImaGenome to our refined version. The left column indicates the detailed operation.

## 6. Grounded Report Refinement Details

### 6.1. Transformation and Distribution of Anatomical Regions

As we said in Section 3.1.1, we provide detailed operations to transform anatomical regions from Chest ImaGenome to our GEMeX. The process is summarized in Table 8. The resulting anatomical region distribution corresponding to each sentence is shown in Figure 3. Overall, there are 30 regions, and the merged area occupies a large proportion, such as “bilateral lung” and “bilateral hilar structures”.

### 6.2. Prompt for Grounded Report Refinement

Here, we provide detailed instructions to refine reports with medical LLM, as we elaborated in Section 3.1.2. The prompt is shown in Table 9, where we add clinical guidance (like (2) (4) (5) (6)) and split and re-written requirements (*e.g.*, (3)) to ensure correct sentence-region correspondence. Moreover, we provide some manually labeled pairs as demonstrations (*i.e.*, “here are some cases”) for in-context learning, aiming to improve overall performance.

## 7. Benchmark Details

### 7.1. Distribution Analysis of Question and Reason Lengths Across Data Splits

We provide a detailed distribution of question and reason lengths across data splits, as presented in Figure 4. It can be seen that under different data splits, the distributions of question (reason) lengths are generally similar. Furthermore, from the perspective of reason, the reason lengths mostly fall between 60 and 150, demonstrating the level of detail in the reasons as textual explanations.

### 7.2. Word Frequency Analysis of Questions and Reasons

Besides providing length distribution, we also explore the frequency of words from both questions and reasons, as shown in Figure 5. From the left part (regarding questions), we can observe that the majority of words are question-related terms, such as “what”, “which”, “is”, and “are”. Additionally, some disease-related terms, such as “abnormality”, “findings”, and “pleural effusion”, are also quite common. Lastly, content words related to the questions, such

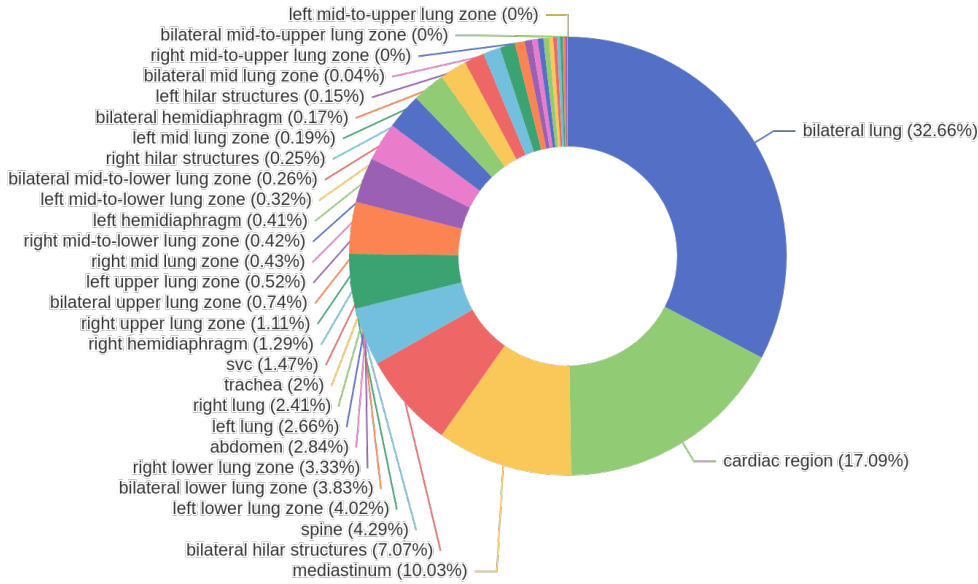


Figure 3. Distribution of anatomical regions corresponding to each sentence after transformation from the Chest ImaGenome dataset.

```

messages = [{"role": "system", "content":
f"“You are a helpful chest X-ray radiologist. Given an input sentence, your task is to map it to an anatomical region on X-ray for better observation from a redefined list [right lung, cardiac silhouette,..., bilateral lower lung zone]. Here are some rules: (1) If there is no corresponding region for this sentence, leave it out. (2) If the sentence describes the overall anatomical characteristics without specifying a particular region, you can choose “bilateral lung” as its region. For example, “No focal consolidation, pleural effusion or pneumothorax is present”：“bilateral lung”. (3) One sentence can only correspond to one region. If a sentence’s main symptom involves several anatomical regions, rephrase it into multiple sentences with corresponding regions. Note that all derived sentences must be syntactically complete, not phrases (i.e., containing a subject and a predicate at least). For example: “The cardiomeastinal silhouette is normal.” can be segmented into “The cardiac silhouette is normal.”：“cardiac region”, “The mediastinal silhouette is normal.”：“mediastinum”, where “cardiomeastinal” corresponds to the “cardiac region” and “mediastinum”. (4) Small (tiny) pleural effusion (fluid) usually appears in the lower lung zone, a moderate pleural effusion appears in the mid-to-lower lung zone, and a large (substantial) pleural effusion can even occupy the entire lung. If the severity (like small, moderate and large) is not indicated, output the left lung or right lung directly. (5) The main anatomical region for observing pulmonary venous is the bilateral hilar structures on the X-ray. (6) The region where the atrium and ventricle can be observed is the cardiac region. Here are some cases: (1)... (2)... (3)... (4)... Organize your output in a json formatted as DictStr(sentence):Str(region), without other words.”}]

messages += [{"role": "user", "content": "Input: “Bibasilar atelectasis is seen without discrete focal consolidation.”"}

```

Table 9. Our proposed prompt for refining sentence-region pairs.

as “regions”, “evidence”, and “size”, are frequently mentioned. These demonstrate the diversity of questions; On the right, we show the word cloud of reasons. It can be seen that the vocabulary mainly falls into two categories: one is related to diseases or anatomical regions, such as “normal”, “heart”, and “pleural”, and the other consists of words used to convey explanations, such as “indicates” and “states”.

### 7.3. Distribution of Question Content Types

We also conduct a statistical analysis about the types of question content that are summarized by GPT-4o itself during VQA generation. The results are shown in Figure 6. It can be observed that under different data splits (i.e., training, valid, and test), the distribution of question content is quite similar. Among them, “abnormality”, “disease”, and “location” account for over 85%, while the remaining portion mainly includes “cause”, “size”, “severity”, and “implication”, which demonstrates the diversity of questions.



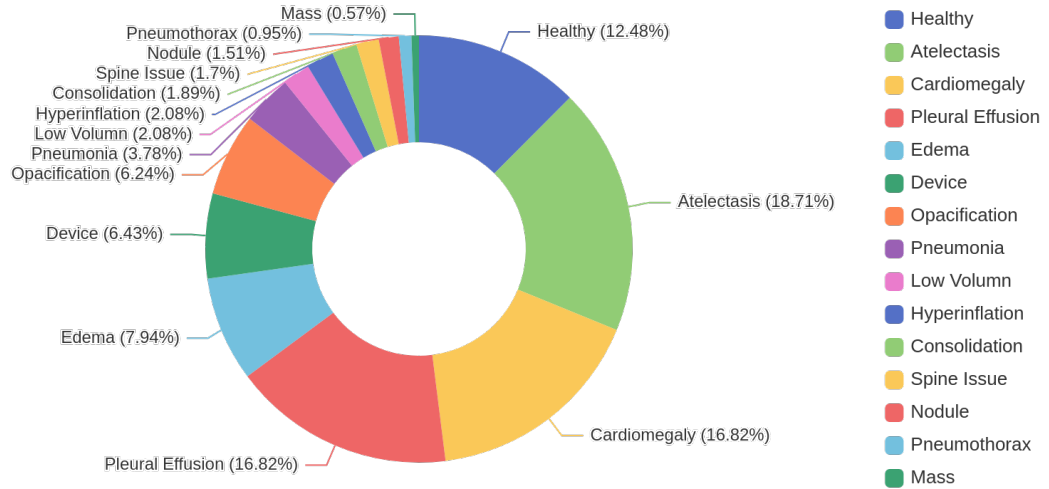


Figure 7. The distribution of normality and abnormality contained in images from the test set of our GEMeX.

#### 7.4. Distribution of Clinical Observations

We manually clean the test set according to the clinical observations present in chest X-ray images. As shown in Figure 7, we plot the distribution of normality and abnormality contained in images. The original distribution of MIMIC-CXR, characterized by a high proportion of healthy samples, introduces a significant bias that affects model performance [33]. To mitigate this issue, we selectively preserve only a small proportion of healthy samples (around 12.48%) during manual cleaning. Simultaneously, we ensure that clinically important observations occupy a substantial proportion, such as “atelectasis”, “cardiomegaly”, “edema”, and “pleural effusion” [19]. Additionally, common diseases or observations like “pneumonia”, “opacification”, and “pneumothorax” are also included.

#### 7.5. LVLMS Introduction

Besides fine-tuning a task-oriented model, we perform a zero-shot evaluation on our GEMeX dataset across the other 10 LVLMS, with 5 in the general domain and the other 5 in the medical domain:

- **In the General Domain:** LLaVA-v1 [35] and Mini-GPT4-v1 [57] are two pioneering works, achieving remarkable results in multimodal tasks; mPLUG-Owl [48] is a multimodal model from the mPLUG series focused on visual-language tasks; LLaVA-v1.5 [34] is an improved version of LLaVA-

v1 with enhancements in multimodal alignment, accuracy, and efficiency; GPT-4o-mini is a smaller, optimized version of GPT-4 [1] intended for lighter computational environments. Note that we did not test GPT-4o because its safety protection policy prohibits it from analyzing medical images.

- **In the Medical Domain:** LLaVA-Med-v1 [26] is designed specifically for medical applications based on LLaVA-v1 and LLaVA-Med-v1.5 [26] is an advanced version; MiniGPT-Med [3] is a medical version of Mini-GPT4 [57]; XrayGPT [40] is a specialized GPT model for interpreting chest X-rays; RadFM [43] is a radiology foundation model.

A chat between a curious human and an artificial intelligence assistant. The assistant gives helpful, detailed, and polite answers to the human's questions. Input an open-ended question, and the assistant will output its answer with a detailed reason and corresponding visual location.\n\n### Human:<image>\n What abnormalities are observed in the left lower lung zone?\n### Assistant: <answer>Linear atelectasis. <reason>The CXR indicates that the lungs are clear except for linear atelectasis located specifically at the left base. <location>[[126, 110, 203, 167]]\n###

Table 10. An input sample of open-ended questions

A chat between a curious human and an artificial intelligence assistant. The assistant gives helpful, detailed, and polite answers to the human's questions. Input a closed-ended question, and the assistant will output its answer (yes or no) with a detailed reason and corresponding visual location.\n\n### Human:<image>\n Are there any lung abnormalities present in this CXR?\n### Assistant: <answer>No. <reason>The CXR clearly shows that the lungs are clear, indicating no lung abnormalities. <location>[[30, 34, 185, 178]]\n###

Table 11. An input sample of closed-ended questions

A chat between a curious human and an artificial intelligence assistant. The assistant gives helpful, detailed, and polite answers to the human's questions. Input a single-choice question, and the assistant will output its answer (an option) with a detailed reason and corresponding visual location.\n\n### Human:<image>\n Which of the following is absent in this CXR? <choices>: [A: Pulmonary edema, B: Pleural effusion, C: Pneumothorax, D: All of the above]\n### Assistant: <answer>D <reason>The CXR shows that there is no pulmonary edema, effusion, or pneumothorax present. <location>[[48, 48, 175, 180]]\n###

Table 12. An input sample of single-choice questions

## 7.6. Input Samples for the Proposed Fine-tuning

We here provide some input samples for a better understanding of how to fine-tune LLaVA-Med [26] on our GEMeX. An input sample of open-ended questions can be seen in Table 10; An input sample of closed-ended questions can be seen in Table 11; An input sample of single-choice questions can be seen in Table 12; An input sample of multi-choice questions can be seen in Table 13.

## 8. More Case Studies

Here, we present more questions with answers from GPT-4o-mini, LLaVA-Med, and our fine-tuned LLaVA-Med-GEMeX, for better understand our dataset

A chat between a curious human and an artificial intelligence assistant. The assistant gives helpful, detailed, and polite answers to the human's questions. Input a multi-choice question, and the assistant will output its answer (some options) with a detailed reason and corresponding visual location.\n\n### Human:<image>\n What abnormalities are mentioned regarding the lung fields? <choices>: [A: Clear lung fields, B: Atelectasis, C: Effusions, D: Congestion]\n### Assistant: <answer>[B, C] <reason>The CXR shows bibasilar atelectasis and small pleural effusions. There is no impressive congestion shown. <location>[[26, 119, 217, 183]]\n###

Table 13. An input sample of multi-choice questions

GEMeX and the corresponding performance of LVLMS.

- We first present some cases of **open-ended questions**, as in Table 14. It can be seen that our fine-tuned model can generally provide correct (or partially correct) answers and identify relatively accurate visual locations. However, other models fail to deliver both precise textual answers and accurate visual positions simultaneously.
- Furthermore, we provide some cases from **closed-ended questions** in Table 15. Although LLaVA-Med can correctly answer the first two questions, it fails to provide visual grounding. For the third question, GPT-4o-mini provides a correct answer, but there is a discrepancy between its grounded visual location (mediastinum) and the ground truth (cardiac region). In contrast, our fine-tuned model can provide both correct answers and accurate visual grounding.
- Next, we show three cases of **single-choice questions**, presented in Table 16. Overall, GPT-4o-mini and LLaVA-Med demonstrate insufficient image understanding capabilities. For instance, in the third example (CASE III), both models incorrectly identify pleural effusion on both sides, whereas it is actually present only in the left lower lung. In comparison, the fine-tuned model shows significant improvement in visual understanding, as evidenced by the grounding results.
- Finally, some cases from **multi-choice questions** are illustrated in Table 17. It can be observed that multi-choice questions are generally more challenging. GPT-4o-mini can only partially identify the correct options; LLaVA-Med tends to answer questions directly based on the question. For example, in all CASEs, it outputs all textually corresponding answers and provides seemingly reasonable explanations, but some of these answers are incorrect when judged based on visual content; The fine-tuned model may also make analytical errors. In CASE III, it incorrectly determines the presence of pleural effusion.



Open-ended questions from GEMeX:

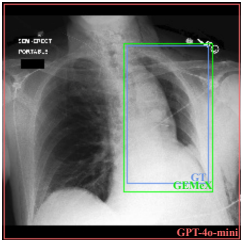
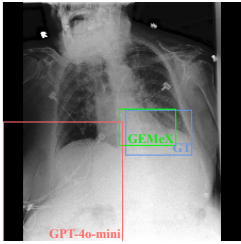
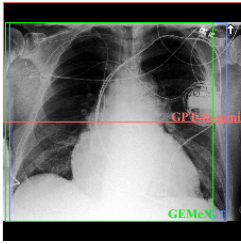
	CASE I  (Bbox predicted by each model)	CASE II  (Bbox predicted by each model)	CASE III  (Bbox predicted by each model)
<i>Question</i>	What might be the cause of the over-expansion of the right lung?	What disease is indicated at the left lung base?	What is the condition of the lungs in this CXR?
<i>Ground Truth</i>	<Answer>: Compensatory hyperinflation due to left lung removal. <Reason>: After a pneumonectomy, the remaining lung may overexpand to compensate for the <b>loss of the left lung</b> .	<Answer>: Atelectasis and/or pulmonary edema. <Reason>: The increased opacity at the left lung base suggests either atelectasis or a combination of atelectasis and pulmonary edema.	<Answer>: Clear. <Reason>: The CXR indicates that the lungs appear clear without definite signs of pneumonia or congestive heart failure (CHF).
GPT-4o-mini	<Answer>: The overexpansion of the right lung may be caused by conditions such as a right-sided pneumothorax or chronic obstructive pulmonary disease (COPD) (✗). <Reason>: Overexpansion can occur when air enters the pleural space (as in pneumothorax) or when there is an obstruction that prevents air from leaving the lung, causing it to become hyperinflated. In COPD, the lung tissue loses elasticity, leading to overinflation. <GPTScore>: 44.44	<Answer>: Possible pneumonia or pleural effusion (✗). <Reason>: The left lung base shows increased opacity, which may indicate fluid accumulation (pleural effusion) or consolidation (pneumonia). These conditions often present as areas of increased density on chest X-rays. <GPTScore>: 55.56	<Answer>: The lungs appear to have a significant opacity, suggesting possible fluid accumulation or consolidation (✗). <Reason>: The central area of the chest X-ray shows increased density, which may indicate the presence of pleural effusion or other pathological processes affecting lung visibility. The clear outlines of the lungs are obscured, which is not typical in a healthy CXR. <GPTScore>: 33.33
LLaVA-Med	<Answer>: The overexpansion of the right lung with a mediastinal shift to the left could be caused by various factors, such as a buildup of air, fluid, or pressure within the lung cavity. This can be due to conditions like pneumothorax (collapsed lung), pleural effusion (fluid buildup around the lungs), or a mass causing pressure on the lung (✗). It's important to consider the patient's clinical history, symptoms, and additional imaging findings to determine the exact cause of the overexpansion and mediastinal shift. <GPTScore>: 55.56	<Answer>: The image shows left lung base fibrocystic disease (✗), which is a lung condition characterized by the presence of fibrous and cystic tissue in the lung base. <GPTScore>: 22.22	<Answer>: In this post-operative chest X-ray (CXR), the lungs appear to be clear and without any signs of infection (✓). <GPTScore>: 77.78
LLaVA-Med-GEMeX	<Answer>: Possible chronic lung disease or compensatory mechanism (✓). <Reason>: Overexpansion of the lung can be due to chronic lung diseases or compensatory mechanisms, especially <b>after a left lobectomy</b> (✓). <GPTScore>: 66.67	<Answer>: Atelectasis (✓). <Reason>: The CXR shows moderate atelectasis at the left lung base (✓), which is a collapse or incomplete expansion of the lung. <GPTScore>: 77.78	<Answer>: Clear. <Reason>: The CXR indicates that the lungs are clear with normal pulmonary vasculature (✓). <GPTScore>: 88.89

Table 14. Open-ended questions from GEMeX answered by GPT-4o-mini, LLaVA-Med, and our fine-tuned LLaVA-Med-GEMeX.

Closed-ended questions from GEMeX:

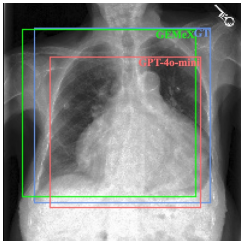
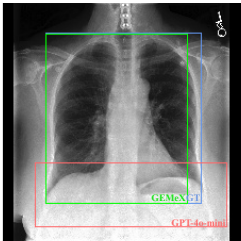
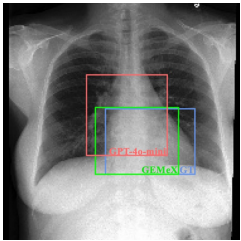
	<p><b>CASE I</b></p>  <p>(Bbox predicted by each model)</p>	<p><b>CASE II</b></p>  <p>(Bbox predicted by each model)</p>	<p><b>CASE III</b></p>  <p>(Bbox predicted by each model)</p>
<i>Question</i>	Are there signs of pneumonia in this CXR?	Is there any pleural effusion present in the CXR?	Is the heart size abnormal in this CXR?
<i>Ground Truth</i>	<Answer>: No. <Reason>: The CXR explicitly states that there is no evidence of pneumonia, indicating clear lung fields.	<Answer>: No. <Reason>: The CXR explicitly states that there is no pleural effusion.	<Answer>: No. <Reason>: The CXR indicates that the heart size is within normal limits.
GPT-4o-mini	<Answer>: Yes. <Reason>: The chest X-ray shows areas of increased opacity, which may indicate the presence of fluid or consolidation (X) typically associated with pneumonia. <GPTScores>: 37.50	<Answer>: Yes. <Reason>: The presence of pleural effusion is indicated by the blunting of the costophrenic angles and the increased opacity in the lower lung fields (X), suggesting fluid accumulation in the pleural space. <GPTScores>: 20.00	<Answer>: No. <Reason>: The heart size appears to be within normal limits (✓) based on the overall silhouette and the ratio of the heart to the thoracic cavity. <GPTScores>: 100.00
LLaVA-Med	<Answer>: No, there are no signs of pneumonia in this chest X-ray (✓). <GPTScores>: 87.50	<Answer>: No, there is no pleural effusion present in the chest X-ray (CXR) (✓). <GPTScores>: 100.00	<Answer>: Yes, the heart size in this chest X-ray appears to be abnormally enlarged (X). This is referred to as cardiomegaly. <GPTScores>: 20.00
LLaVA-Med-GEMeX	<Answer>: No. <Reason>: The CXR indicates no focal consolidation, which rules out pneumonia (✓). <GPTScores>: 100	<Answer>: No. <Reason>: The CXR clearly states that there is no pleural effusion (✓). <GPTScores>: 100.00	<Answer>: No. <Reason>: The heart is described as normal in size (✓). <GPTScores>: 100.00

Table 15. Closed-ended questions from GEMeX answered by GPT-4o-mini, LLaVA-Med, and our fine-tuned LLaVA-Med-GEMeX.

Single-choice questions from GEMeX:

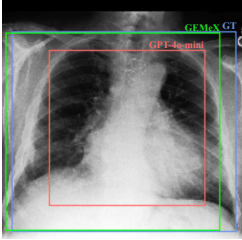
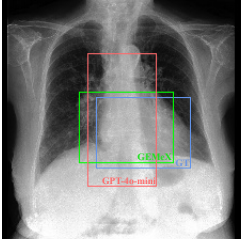
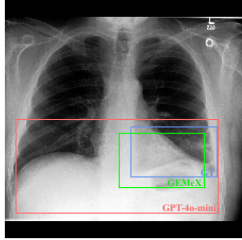
	CASE I 	CASE II 	CASE III 
	(Bbox predicted by each model)	(Bbox predicted by each model)	(Bbox predicted by each model)
<i>Question</i>	What is the overall condition of the lungs based on the CXR? Choices: [A: Clear, B: Consolidated, C: Effused, D: Thickened]	What does the CXR indicate about the heart size? Choices: [A: Normal, B: Mild cardiomegaly, C: Moderate cardiomegaly, D: Severe cardiomegaly]	Which regions are assessed for pleural effusion in this CXR? Choices: [A: Right lower lung zone, B: Left lower lung zone, C: Cardiac region, D: Bilateral lung]
<i>Ground Truth</i>	<Answer>: A. <Reason>: The CXR indicates that the lungs are clear of consolidation or effusion, although right pleural-based thickening at the base.	<Answer>: C. <Reason>: The CXR indicates unchanged moderate cardiomegaly.	<Answer>: B. <Reason>: The pleural effusion is specifically noted in the left lower lung zone.
GPT-4o-mini	<Answer>: B. <Reason>: The presence of increased opacity in the lung fields suggests consolidation, indicating that the lungs are not clear and may have fluid or solid material in the alveoli (✗). <GPTScore>: 33.33	<Answer>: B. <Reason>: The CXR shows an enlarged heart silhouette, indicating mild cardiomegaly. The heart appears larger than normal but not excessively so (✗). <GPTScore>: 55.56	<Answer>: D. <Reason>: Pleural effusion can accumulate in the lower lung zones, and both sides of the chest. The bilateral lung regions are crucial for evaluating pleural effusion (✗). <GPTScore>: 66.67
LLaVA-Med	<Answer>: The chest X-ray (CXR) shows bilateral diffuse interstitial thickening, which means that both lungs have a thickened appearance in their interstitial areas (✗). This finding can be associated with various lung conditions, such as infections, inflammation, or fibrosis. It is important to consider the patient's clinical history and symptoms, as well as consult a healthcare professional for a thorough evaluation and proper diagnosis of the underlying cause of these findings. <GPTScore>: 37.50	<Answer>: The CXR indicates that there is mild cardiomegaly, which means that the heart appears slightly enlarged (✗). <GPTScore>: 44.44	<Answer>: In this chest X-ray (CXR), the regions assessed for pleural effusion include the right lower lung zone, the left lower lung zone, the cardiac region, and the bilateral lung (✗). <GPTScore>: 50.00
LLaVA-Med-GEMeX	<Answer>: A. <Reason>: The CXR indicates that the lungs are otherwise clear except for the noted pleural thickening (✓). <GPTScore>: 88.89	<Answer>: C. <Reason>: The CXR indicates moderate cardiomegaly (✓). <GPTScore>: 100.00	<Answer>: B. <Reason>: The CXR specifically indicates that trace pleural effusion is difficult to exclude in the left lower lung zone (✓). <GPTScore>: 87.50

Table 16. Single-choice questions from GEMeX answered by GPT-4o-mini, LLaVA-Med, and our fine-tuned LLaVA-Med-GEMeX.

Multi-choice questions from GEMeX:

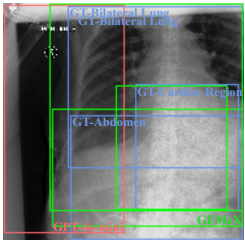
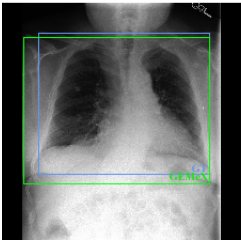
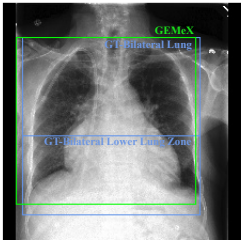
	CASE I 	CASE II 	CASE III 
	(Bbox predicted by each model)	(Bbox predicted by each model)	(Bbox predicted by each model)
<i>Question</i>	What regions on the X-ray indicate abnormal findings? Choices: [A: Bilateral lung, B: Cardiac region, C: Abdomen, D: Spine]	Which findings indicate abnormal lung conditions? Choices: [A: Mild interstitial abnormality, B: Hyperinflation, C: Focal consolidation, D: No pleural effusion]	Which observations rule out serious lung conditions in this CXR? [A: No pneumonia, B: No lung nodules, C: No pleural effusions, D: No lymphadenopathy]
<i>Ground Truth</i>	<Answer>: [A, B, C]. <Reason>: <b>The bilateral lung shows pleural effusion</b> , the cardiac region shows enlargement, <b>and the abdomen shows the nasogastric tube</b> . The spine is normal.	<Answer>: [A, B]. <Reason>: <b>Mild interstitial abnormality and hyperinflation indicate abnormal lung conditions</b> . There is no focal consolidation.	<Answer>: [A, B, D] <Reason>: <b>The CXR shows no pneumonia, lung nodules, or lymphadenopathy, which rules out serious lung conditions</b> . However, there are mild bilateral pleural effusions.
GPT-4o-mini	<Answer>: [A: Bilateral lung]. <Reason>: <b>The bilateral lung region shows potential abnormalities such as opacities or other irregularities that may indicate pathology (X)</b> . <GPtScore>: 37.50	<Answer>: [A, B, C]. <Reason>: <b>Mild interstitial abnormality, hyperinflation (✓), and focal consolidation (X) are all findings that indicate abnormal lung conditions</b> . <GPtScore>: 66.67	<Answer>: [A, B, C, D]. <Reason>: <b>The absence of pneumonia, lung nodules, pleural effusions (X), and lymphadenopathy (✓) in the chest X-ray suggests that there are no serious lung conditions present</b> . Each of these findings is associated with significant lung pathology, and their absence helps rule out serious issues. <GPtScore>: 62.50
LLaVA-Med	<Answer>: The chest X-ray shows abnormal findings in multiple regions. The left side of the image indicates <b>bilateral lung abnormalities, which could be related to lung issues such as infection, inflammation, or other lung conditions (X)</b> . The right side of the image shows abnormal findings in the cardiac region, which may suggest issues with the heart or surrounding structures (✓). <b>The lower part of the image reveals abnormal findings in the abdomen, which could be related to gastrointestinal or other abdominal issues (✓)</b> . Lastly, the spine region also shows abnormal findings, which could be related to spinal issues or other back-related problems. <GPtScore>: 50.00	<Answer>: The chest x-ray shows findings A, B, and C, which indicate abnormal lung conditions. <b>These findings are likely a combination of interstitial thickening, hyperinflation (✓), and focal consolidation (X)</b> . These abnormalities can be associated with various lung conditions, such as chronic obstructive pulmonary disease (COPD), asthma, or other respiratory disorders. <GPtScore>: 55.56	<Answer>: The image shows a chest X-ray that demonstrates the absence of certain conditions, which are marked as B on the image. <b>These conditions include pneumonia, lung nodules, lymphadenopathy (✓), and pleural effusions (X)</b> . This means that the chest X-ray does not show any signs of these lung conditions, ruling them out based on the image. <GPtScore>: 62.50
LLaVA-Med-GEMeX	<Answer>: [A, B, C]. <Reason>: <b>The bilateral lung shows interstitial opacities (X)</b> , the cardiac region shows enlargement (✓), <b>and the abdomen shows the feeding tube location (✓)</b> . <GPtScore>: 87.50	<Answer>: [A, B]. <Reason>: The CXR shows <b>mild interstitial abnormality and hyperinflation (✓)</b> as abnormal lung conditions. <GPtScore>: 88.89	<Answer>: [A, B, C, D]. <Reason>: The CXR indicates <b>the absence of pneumonia, lung nodules, pleural effusions (X), and lymphadenopathy (✓)</b> . <GPtScore>: 62.50

Table 17. Multi-choice questions from GEMeX answered by GPT-4o-mini, LLaVA-Med, and our fine-tuned LLaVA-Med-GEMeX.